The Role of Evection in Optical Measurements of Light Beam Deflection from the Sun's Disk (the Einstein Effect)

Sergey N. Shapovalov

SCC RF Arctic and Antarctic Research Institute. 38 Bering St., St. Petersburg 199397, Russia
E-mail: shapovalov@aari.ru, tel. +7 (812) 3373157

The relationship between the optical results of light beam deflection from the disk of the Sun ($\delta\varphi$) obtained during observations of the total solar eclipses, from 1919 till 1973, and the evection, the major perturbation from the Sun, based on the theory of the Moon's motion, is analysed. The dependence of $\delta\varphi$ upon the temporal changes of the evection was found. The expected $\delta\varphi$ optical results for the total solar eclipses, for the period from 22.09.2003 till 29.12.2103, were calculated. Based on the comparison of calculated evection values with fluctuations of intensity of solar radiation within 603–607 nm range obtained through the spectral observations on solar radiation in Antarctica, the modulatory role of the evection in deflecting the light beam at the near-Earth space was concluded.

Optical measurements of the star beam deflection from the Sun disk were performed by a number of researchers during the total solar eclipses, from 29.05.1919 till 30.06.1973, with the purpose of checking the $\delta\varphi$ angle value (1.75″) obtained by Einstein, following his development of the General Theory of Relativity (GTR) [1]. In case the radio measurements only are considered in the practical estimates of the Einstein effect, $\delta\varphi$ values match with the theory within 1% range [2]. For example, an average value of 1.73″(±0.07″) was obtained in radar measurements of Mercury, Venus and Mars, whereas measurements of quasars and pulsars using radio interferometry produced an estimate of 1.76″(±0.08). Deflection of the beam from the Sun disk is described by the equation:

$$\delta\varphi = -\frac{4GM_{\odot}}{R_{\odot}c^2}\,, \qquad (1)$$

where the "minus" sign corresponds to the deflection of the beam to the center of the Sun; $G = 6.67{\times}10^{-11}$ H×m^2/kg^2 is the gravitational constant; $M_{\odot} = 1.99{\times}10^{30}$ kg is the mass of the Sun; $c = 3{\times}10^8$ m/s is the speed of light; $R_{\odot} = 6.96{\times}10^8$ m is the radius of the Sun.

Based on the optical observations of the eight total solar eclipses, the author's average result together with a confidence interval of measurements makes $\delta\varphi = 1.83 \pm 0.40$, and the recalculated measurement result is $\delta\varphi = 2.0 \pm 0.13$, which, in view of the low accuracy and the considerable spread of measurements, is consistent with the GTR. According to the published data [3–10], the results of $\delta\varphi$ optical measurements for the total solar eclipses observed from 1919 till 1973 were as follows:

29.05.1919: (1.98, 0.93, 1.61),

21.09.1922: (1.42, 1.75, 2.16, 1.72, 1.83, 1.77),

09.05.1929: (2.24),

19.06.1936: (2.73, 2.13, 1.28),

20.05.1947: (2.01),

25.02.1952: (1.70, 1.82),

02.10.1959: (2.17),

30.06.1973: (1.66).

Observations referring to the date 19.06.1936 should be considered as ineffectual, since the absolute value error exceeds 200%. To date, the list of known errors includes:

— Deviation of the Sun's shape from the sphericity, $9.2'' {\times} 10^{-2}$;

— The Earth's motion along the ecliptic ($2.88'' {\times} 10^{-2}$);

— Beam refraction in the atmosphere of the Sun (0.004″);

— Refraction and dispersion in the Earth atmosphere (0.01″–0.1″);

— Offset of the observer from the Sun-Moon-Earth line;

— The influence of the gravitational field of the Moon and the Earth during the total eclipse event, by an addition to the relativistic beam deflection ($5.8'' {\times} 10^{-4}$);

— Wavelength dependence of the light beam ($2.5'' {\times} 10^{-4}$);

— Dependence on solar activity;

— Astroclimatic characteristics of a particular observation station;

— Additive error caused by inaccurate scale matching between the day and night astroimages (0.25″).

It should be noted that through the history of $\delta\varphi$ measurements the list of errors has expanded considerably; however, the accuracy of estimates is not yet improved. Summing the values of all the errors, the magnitude of the total correction is apparently insignificant. Therefore, dispersion of $\delta\varphi$ results is probably due to the influence of some unknown factors.

The major solar-induced disturbances are described by terms in the formula of the geocentric ecliptic longitude of the Moon [11, 12]. Full description of this formula includes 1,500 terms [13], where evection, variation and annual inequality are the most important. When limited to the largest

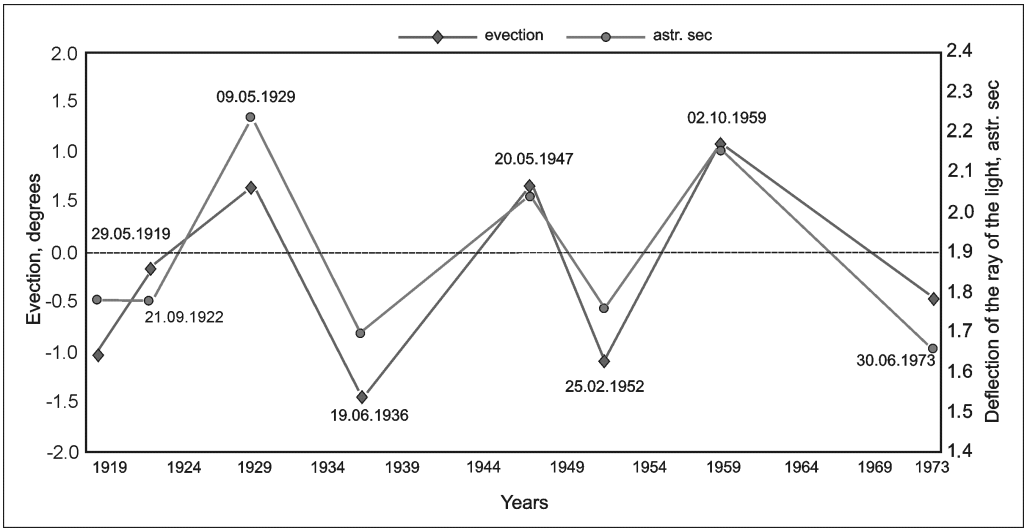

Fig. 1: Comparison of the evection angle values with the results of optical measurements taken as average values and excluding errors for the dates of the total solar eclipses, 1919–1973.

in amplitude terms, the formula is as follows:

$$\lambda = L + 6.289^\circ \sin l - 1.274^\circ \sin(l - 2D) + \\ + 0.658^\circ \sin 2t + 0.214^\circ \sin 2l - \\ - 0.186^\circ \sin l' - 0.114^\circ \sin 2F\,, \qquad (2)$$

where L is the mean longitude (void of the periodic disturbances) of the Moon in the orbit, l, D, l', F are the main arguments in the lunar theory.

In the first five inequalities of the formula (2), the terms bearing coefficients 6.289 and 0.214 are determined by ellipticity of unperturbed (Keplerian) orbit, whereas the terms with coefficients 1.274 (evection, 31.8 days), 0.658 (variation, 14.8 days) and 0.186 (annual inequality, 186.2 days) are caused by gravitational perturbations from the Sun. The periods of these inequalities, according to the theory of motion of the Moon, exist in the short-period nutation of the Earth's axis, as well [14]. In this paper we consider the contribution of the evection, the main and the largest in amplitude perturbation from the Sun, as the most significant deviation of the true motion of the Moon from its motion defined by Kepler's laws. Evection was discovered by Ptolemy (2AD) when observing the Moon in the 1st and 3rd quarters (in quadrature points). The physical explanation of the evection was developed by Newton. Evection can be represented as a difference in the equation of the center [13] generated by the term $1.274^\circ \sin(l - 2D)$:

$$e_\odot = 5.02 \sin l + 0.214 \sin 2l\,, \qquad (3)$$

$$e_\odot = 7.56 \sin l + 0.214 \sin 2l\,. \qquad (4)$$

This effect is determined by the gravitational influence of the Sun to the Moon. In syzygial points of the lunar orbit (new moon and full moon), this term is subtracted from the senior term of the equation (3), and it is added in quadrature. During the new moon and full moon, $2D = 0^\circ$, or 360° (3), which is the same in the context of trigonometric functions. In the first and last quarters, $D = 90^\circ$, or 270° (4). So, the known manifestations of the evection in the near-Earth space motivated the studies of its contribution to the results of $\delta\varphi$ assessments obtained during observations of the total solar eclipses, from 1919 till 1973.

The *evection* values were calculated upon the Julian dates of the total solar eclipses. Fig. 1 shows a comparison of the evection angle values with the results of optical measurements taken as average values and excluding errors for the dates of the total solar eclipses. Anomalous results 0.93″ (1919) and 2.73″ (1936) were omitted from the calculations of average values, as they fell outside the range of average result and the confidence interval of all measurements.

Fig. 2 shows the distribution of dependency of optical results from the evection. Continuous curve, which includes 0.93″ (1919) and 2.73″ (1936) values, represents averaging of results depending on the evection and is described as:

$$\delta\varphi(M) = 1.7227 + 0.2058\,x + 0.3163\,x^2. \qquad (5)$$

The dotted curve, which excludes 0.93″ (1919) and 2.73″ (1936) values, represents averaging of results depending on the evection and is described as follows:

$$\delta\varphi(E) = 1.723 + 0.316\,x^2. \qquad (6)$$

As demonstrated in the Figure, $\delta\varphi(M)$ has a lower left-hand shift against $\delta\varphi(E)$ characterized by the term $0.2058\,x$ (5), due to the low values obtained during the observations of 1919 ($\delta\varphi = 0.93''$) and 1936 ($\delta\varphi = 1.28''$). According to $\delta\varphi(E)$ distribution in Fig. 2, deflection of beams in

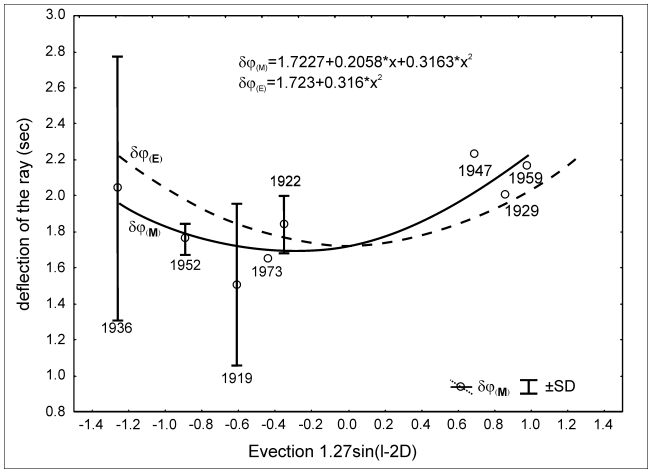

Fig. 2: Distribution of $\delta\varphi$ values according to the *evection* values, 1919–1973: $\delta\varphi(M)$ averaged optical results dependent on the evection, 0.93″ (1919) and 2.73″ (1936) values included; $\delta\varphi(E)$ averaged optical results dependent on the evection, 0.93″ (1919) and 2.73″ (1936) values excluded.

the evection extremes (±1.274°) should correspond to $\delta\varphi \approx 2.25 \pm 10\%$, and to $\delta\varphi \approx 1.72$ in case of 0, i.e., conform to the Einstein result. Using the expression (6), the expected $\delta\varphi$ values calculated for optical observations at the dates of the total solar eclipse, from 23.11.2003 till 29.12.2103, are presented in Table 1.

Along with the deviations in the motion of the Moon from the Keplerian orbit and the short-period nutation of the Earth axis, the evection mechanism is detected in spectral zenith observations of the atmosphere at Novolazarevskaya station (Antarctica). These observations are aimed to investigate the fluctuations of energy and intensity of scattered solar UV radiation under the 11-year SA cycle. Measurements of fluctuations are recorded in the following ranges: 303–305 nm, 331–332.5 nm, 329.5–334 nm, 336–345 nm, 297–307 nm, 321–331 nm, 297–330 nm, and 603–607 nm, during the polar summer (September – February). Detailed description of the methodology of observations is cited in [15].

To test the influence of the evection factor on variations of the light flux, fluctuations measurements in the range of 603–607 nm (as the most proximate band to the central part of the solar spectrum) were selected from the available set of registered channels. Based on the observations during the polar summer 2007–2008 and 2008–2009, data analysis of the intensity channel was performed, in average daily standard deviation (SD) units, to build the time series and provide temporal comparison with the calculated values of the evection. Figs. 3 and 4 show the distribution pattern of SD values (603–607 nm), to be compared with the evection changes.

The figures show a reasonably good phase and periodic matching between the SD (603–607 nm) dynamics and the evection changes during the polar summer of 2007–2008. However, Fig. 4 shows the broken phase matching at certain

Eclipses	$\delta\varphi(E)$	Eclipses	$\delta\varphi(E)$	Eclipses	$\delta\varphi(E)$
23.11.2003	1.75	26.12.2038	2.02	03.08.2073	2.11
08.04.2005	2.24	21.06.2039	1.82	27.01.2074	2.23
03.10.2005	2.09	15.12.2039	1.72	24.07.2074	2.13
29.03.2006	1.89	30.04.2041	2.23	16.01.2075	2.03
22.09.2006	1.74	25.10.2041	2.01	13.07.2075	1.76
07.02.2008	2.22	20.04.2042	1.81	06.01.2076	1.73
01.08.2008	2.16	14.10.2042	1.72	22.05.2077	2.19
26.01.2009	1.88	28.02.2044	2.22	15.11.2077	2.02
22.07.2009	1.74	23.08.2044	2.09	11.05.2078	1.83
15.01.2010	1.75	16.02.2045	1.89	04.11.2078	1.72
11.07.2010	1.9	12.08.2045	1.74	01.05.2079	1.86
20.05.2012	1.78	05.02.2046	1.74	24.10.2079	1.96
13.11.2012	1.72	02.08.2046	1.98	10.03.2081	1.82
10.05.2013	1.91	11.06.2048	1.74	03.09.2081	1.72
03.11.2013	2.11	05.12.2048	1.75	27.02.2082	1.79
09.03.2016	1.92	31.05.2049	1.89	24.08.2082	2.07
01.09.2016	2.02	25.11.2049	2.17	03.07.2084	1.72
26.02.2017	2.23	20.05.2050	2.22	27.12.2084	1.79
21.08.2017	2.23	30.03.2052	1.91	22.06.2085	1.98
02.07.2019	2.03	22.09.2052	2.01	16.12.2085	2.16
26.12.2019	2.2	20.03.2053	2.23	11.06.2086	2.24
21.06.2020	2.18	12.09.2053	2.2	21.04.2088	1.99
14.12.2020	2.11	24.07.2055	2.11	14.10.2088	2.09
10.06.2021	1.82	16.01.2056	2.19	10.04.2089	2.24
04.12.2021	1.72	12.07.2056	2.19	04.10.2089	2.14
20.04.2023	2.22	05.01.2057	2.02	23.09.2090	1.77
14.10.2023	2.1	01.07.2057	1.83	15.08.2091	2.18
08.04.2024	1.89	26.12.2057	1.73	07.02.2092	2.23
02.10.2024	1.75	11.05.2059	2.23	03.08.2092	2.13
17.02.2026	2.22	05.11.2059	2.01	27.01.2093	1.94
12.08.2026	2.17	30.04.2060	1.82	23.07.2093	1.77
06.02.2027	1.88	24.10.2060	1.72	16.01.2094	1.73
02.08.2027	1.74	20.04.2061	1.86	02.06.2095	2.19
26.01.2028	1.74	13.10.2061	1.96	27.11.2095	1.93
22.07.2028	1.99	28.02.2063	1.81	22.05.2096	1.76
01.06.2030	1.74	24.08.2063	1.72	15.11.2096	1.73
25.11.2030	1.75	17.02.2064	1.79	11.05.2097	1.85
21.05.2031	1.9	12.08.2064	1.98	04.11.2097	2.05
14.11.2031	2.1	22.06.2066	1.74	21.03.2099	1.82
09.05.2032	2.23	17.12.2066	1.8	14.09.2099	1.72
30.03.2033	1.78	11.06.2067	1.89	10.03.2100	1.78
20.03.2034	1.91	06.12.2067	2.17	04.09.2100	2.06
12.09.2034	2.02	31.05.2068	2.24	28.02.2101	2.21
09.03.2035	2.23	11.04.2070	2	15.07.2102	1.72
02.09.2035	2.19	04.10.2070	2.1	08.01.2103	1.79
13.07.2037	2.12	31.03.2071	2.23	04.07.2103	1.97
05.01.2038	2.19	23.09.2071	2.2	29.12.2103	2.22
02.07.2038	2.19	12.09.2072	1.77		

Table 1: Expected $\delta\varphi$ results for the total solar eclipses, from 23.11.2003 till 12.29.2103.

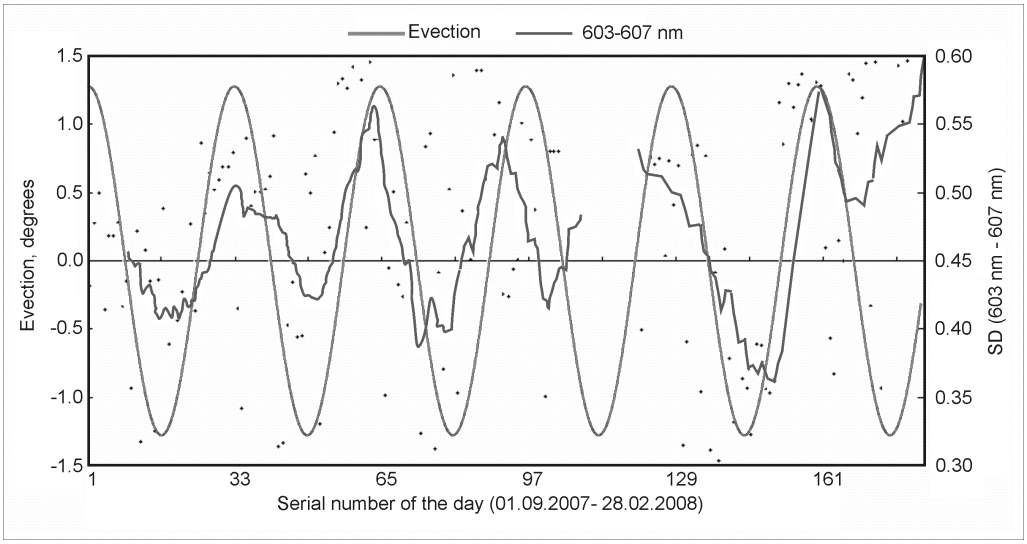

Fig. 3: Comparison of temporal changes in the evection and the average daily standard deviation (SD) of radiation intensity in the 603–607 nm (9 pt. mov. aver.) range, for the period from 01.09.2007 till 28.02.2008.

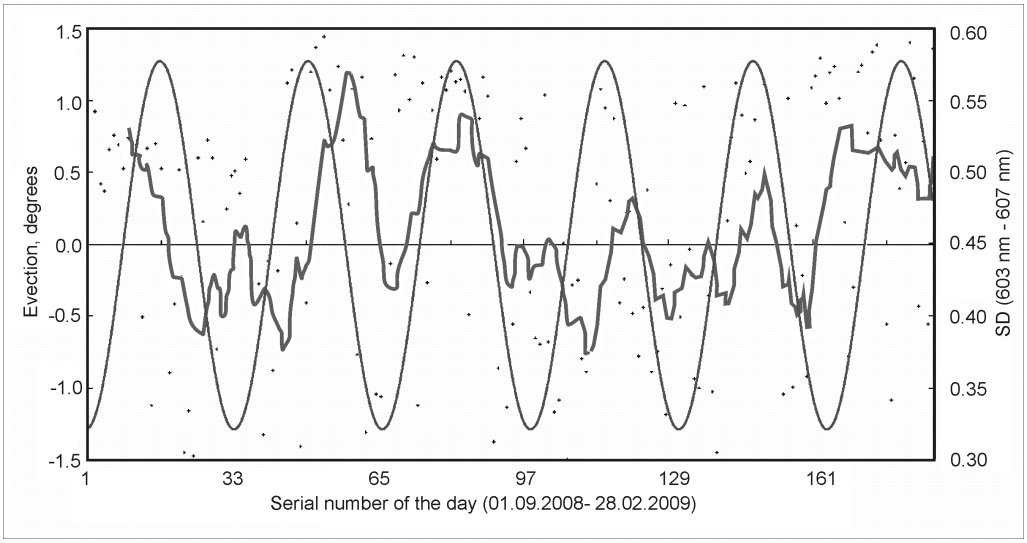

Fig. 4: Comparison of temporal changes in the evection and the average daily standard deviation (SD) of radiation intensity in the 603–607 nm (9 pt. mov. aver.) range, for the period from 01.09.2008 till 28.02.2009.

extended sections. In our view, such failures may be related to the SA stages. Among the above errors, $\delta\varphi$ dependence from SA and astroclimatic characteristics of observation stations remain understudied. Astroclimatic characteristics are determined by the weather conditions and optical properties of the atmosphere and both are connected with the SA manifestations. Although the mechanism of SA effects on the surface layer of the atmosphere remains unclear to date, this connection is revealed by the long-term observations of weather services.

In a brief discussion of relationship between $\delta\varphi$ and the evection, previously disregarded in research practice, a 3-body Einstein model should be mentioned, which considers the Earth and the Moon as point-like objects. This model is undeniable in the evaluation of mass gravitation of the Earth–Moon and the Sun. The major solar disturbances cause deviation from the Keplerian orbit of the Moon motion and, at the same time, deviations in the Earth axis in the short-period nutation (31.8 and 14.8 days), provide periodic gravitational influence on the Earth–Moon system. Obviously, this influence

is manifested in the Einstein effect through the modulation property of optical beams.

Conclusions

— The values of $\delta\varphi$ optical results reveal statistical correlation with the temporal change of the evection;

— In the evection extreme points ($\pm 1.274^\circ$), deflection of optical beams from the solar disk is expected to approach $\delta\varphi \approx 2.25 \pm 10\%$;

— When the evection values $\approx 0^\circ$, it is expected to approach $\delta\varphi = 1.72 \pm 10\%$;

— In conformity with $\delta\varphi(E)$, introduction of correction for the evection into the formula (1) is justified.

Submitted on: April 26, 2013 / Accepted on: May 06, 2013

References

1. Einstein A. *Ann. Phys.*, 1916, Bd.49, 769.
2. Ginzburg V.L. Theoretical physics and astrophysics. Nauka, Moscow, 1980.
3. Crommelin A. Results of the total solar eclipse of May 29 end the relativity theories. *Nature*, 1920, v.104, 280–281.
4. Hopmann J. Die Deutung der Ergebnisse der amerikanischen Einstein expedition. *Phys. Z.*, 1923, Bd.24, No.21/22, 476–485.
5. Eddington A.S. The deflection of light during a solar eclipse. *Nature*, 1919, v.104, no.271, 454.
6. Mikhailov A.A. Einstein's effect observations. *Astronomicheskiy Zhurnal*, 1956, no.33, 912–927.
7. Freundlich E.F., von Kluber H.V., Brunn A. Ergebniss der Potsdamer Expedition zur Beib chtung der Sonnenfinsternis von 1929, Mai 9 die Ablenkung des Lichtes in Schwerefeld der Sonne. *Phys. Ber.*, 1931, No.1, 2838–2839.
8. Schmeidler F. Neuer Versuch einer Messung der relativitischen Lichtablenkung. *Astron. Nachrichten*, 1963, Bd.287, No.1-2, 7–16.
9. Jones B.F. Texas Mauritanian Eclipse Team. Gravitational deflection of light: Solar eclipse of 30 June 1973. I. Description of procedures and final results. *Astron. J.*, 1974, v.81, 452–454.
10. Jones B.F. Gravitational deflection of light: solar eclipse of 30 June 1973. II. Plate reduction. *Astron. J.*, 1974, v.81, 455–463.
11. Astronomicheskiy Ezhegodnik. Part 1. Inst. Appl. Astron., Russian Acad. Sci., St. Petersburg, 1998.
12. Meeus J. Astronomical formulae for calculators. Mir, Moscow, 1988.
13. Brown F.H. Tables of the motion of the Moon. New Hawen, 1919.
14. Kulikov K.A. Rotation of the Earth. Nedra, Moscow, 1985.
15. http://www.aari.nw.ru/clgmi/geophys/data_nvl_ru.html